RESEARCH ARTICLE | MARCH 17 2008

Excimer-based red/near-infrared organic light-emitting diodes with very high quantum efficiency

M. Cocchi; J. Kalinowski; D. Virgili; J. A. G. Williams

Appl. Phys. Lett. 92, 113302 (2008)
https://doi.org/10.1063/1.2898159

Excimer-based red/near-infrared organic light-emitting diodes with very high quantum efficiency

M. Cocchi,[1,a)] J. Kalinowski,[2,b)] D. Virgili,[1] and J. A. G. Williams[3]
[1]*Institute of Organic Synthesis and Photoreactivity, National Research Council of Italy (ISOF-CNR), I-40129 Bologna, Italy*
[2]*Department of Molecular Physics, Gdańsk University of Technology, 80-952 Gdańsk, Poland*
[3]*Department of Chemistry, University of Durham, Durham DH1 3LE, United Kingdom*

(Received 25 January 2008; accepted 25 February 2008; published online 17 March 2008)

Various light output measures of red/near-infrared (NIR) excimer-based organic light-emitting diodes (LEDs) are reported for different cathodes (Al, Al/LiF, Ca, and Ca/PbO_2). By using a selected phosphor (PtL^2Cl) from a series of terdentate cyclometallated efficient phosphorescent Pt(II) complexes, PtL^nCl, as the neat film emitting layer and a Ca/Pb(IV)O_2 cathode, the authors achieve unusually high forward viewing external quantum efficiencies of up to 14.5% photons/electron and a power conversion efficiency of up to 6% at a high emission forward output of 25 mW/cm^2. These are the highest efficiencies reported for a NIR organic LED. Electron tunneling through thin insulating layers of LiF and Pb(IV)O_2 and the difference in band bending at the organic electron transporting layer and the cathode between the samples are used to explain this performance achievement. © *2008 American Institute of Physics*. [DOI: 10.1063/1.2898159]

Considerable achievements in quantum efficiency (QE) and performance have led to the development of organic light-emitting diodes (LEDs) operating in the visible range.[1–3] The extension of efficient organic LEDs into the technologically important near-infrared (NIR) spectral range is a challenge to scientists and engineers. Only recently, the application of generating excimer phosphorescence of neat films made of terdentate cyclometallated Pt(II) complexes has enabled the fabrication of highly efficient [10.7 ± 0.5% photon/electron (ph/e) at current densities as high as 10 mA/cm^2] red/NIR (peaking at 720 nm) organic LEDs.[4] We note that the boundary between visible and infrared radiation is not precisely defined, but according to the International Commission on Illumination (CIE), the first NIR range (IR-A) spans 700–1400 nm. This is the range based on the approximate end of the response of the human eye to that of silicon. Later on, a value of 8.5 ± 0.3% ph/e with monomer electrophosphorescence (peaking at 772 nm) at a very low current density of 0.001 mA/cm^2 and a much lower value of $\approx$3% ph/e at 10 mA/cm^2 have been obtained.[5] The high electroluminescence (EL) QE of excimer-based NIR organic LEDs was ascribed to the high photoluminescence (PL) efficiency of excimeric emission of neat PtL^nCl films and to the confinement of the recombination zone within the emission layer (EML). In those NIR LEDs, a vacuum-evaporated cathode of Ca has been used as an electron-injecting contact.

The present work demonstrates that inserting a layer of LiF or Pb(IV)O_2 with a 0.5 nm thickness between the electron transporting layer (ETL) and metal vacuum-evaporated layers, Al or Ca, respectively, allows us to greatly enhance the electron injection from the cathode, reduce the operating voltage, and improve optical output characteristics, including EL QE and power conversion efficiency. We have chosen a monomer/excimer emitting material PtL^2Cl (Fig. 1) from a group of highly efficient NˆCˆN-coordinated platinum (II) complex phosphors, PtL^nCl (where $n=1-6$ represents various substituents at four positions of the central phenyl ring, CO_2Me for L^2),[6] and fabricated a four-layer LED. The devices fabricated have the following structure: indium tin oxide (ITO)/75 wt % N,N'-diphenyl-N,N' bis(3-methylphenyl)-[1,1′-biphenyl]-4,4′-diamine (TPD): 25 wt % bisphenolpol-*A*-polycarbonate (PC)/100% 4,4′-N,N'-dicarbazole-biphenyl (CBP)/100% PtL^2Cl/100% 3,5-bis[5-(4-tert-butylphenyl)-1,3,4-oxadiazol-2-yl]-benzene (OXA)/different cathodes (Al, Al/LiF, Ca, and PbO_2/Ca). The LED structure and materials used along with their energy level positions are shown in Fig. 1. Neat film emitters made of a terdentate cyclometallated phosphorescent Pt(II) complex (PtL^2Cl) serve as EMLs. They exhibit exclusive red/NIR excimer emission peaking at a wavelength of 700 nm. The LED structure with the Ca/Pb(IV)O_2 cathode reveals unusually high forward viewing external QEs of up to 14.5% ph/e and a power conversion efficiency of 6% at a high emission power output of 25 mW/cm^2. These are the highest figures reported for a NIR organic LED to date. The difference in band bending at the organic ETL and the cathode[7] is used to explain this performance achievement.

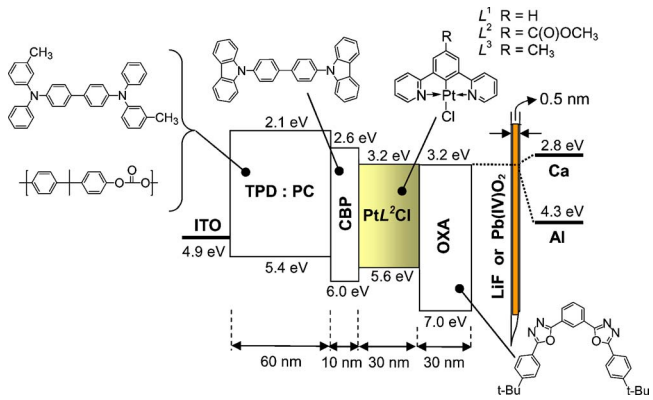

FIG. 1. (Color online) Energy level diagram of the NIR EL devices and molecular structures of the materials used.

a)Electronic mail: cocchi@isof.cnr.it.
b)Electronic mail: kalino@polnet.cc.

The synthesis of PtL^2Cl has been described previously (Ref. 6 and references therein). Commercially available ITO with a sheet resistivity of 20 Ω/□ on glass substrates was used in the device fabrication process. In the device architecture, two hole- and exciton-blocking layers (CBP and OXA) were introduced to confine the electron-hole recombination and emission processes within the emitting layer of neat PtL^2Cl emitters. A 60 nm thick hole transporting layer of [TDP]: [PC (molecular weight, 32 000–36 000)] (Aldrich and Polysciences, Inc., respectively) blend was spun on top of the ITO from a 10 mg/ml dichloromethane solution at room temperature. It was followed by a vacuum-evaporated 10 nm thick hole-blocking layer of CBP. The active, 30 nm thick emissive layer of the Pt complex reported in Fig. 1 was evaporated under a vacuum of 10^{-5} hPa on top of the CBP layer. Subsequently evaporated on them was a 30 nm thick layer of OXA (Syntech), which served as an electron transporting and hole- and exciton-blocking layer. The opposing electrodes of Al, Al/LiF, Ca, or Ca/Pb(IV)O_2 that were used to inject electrons were deposited directly or consecutively (for bi component electrodes) on the ETL of OXA by thermal evaporation *in vacuo*. The thickness of each layer was measured with a Tencor Alpha-Step 200 profilometer. The highest occupied molecular orbital (HOMO) levels were estimated from oxidation potentials. For example, the HOMO level of PtL^2Cl has been determined from the measured oxidation potential $E^{ox}=0.89\pm0.05$ eV in acetonitrile:dichloromethane (9:1) versus standard saturated calomel electrode (SCE), which takes the work function $E^{SCE}=4.7\pm0.15$ eV: $E^{HOMO}=E^{ox}+E^{SCE}=5.6\pm0.2$ eV. It is slightly higher than the value $E^{HOMO}=5.3\pm0.2$ eV calculated from the linear relationship $E^{HOMO}=(1.4\pm0.1)E^{ox}+(4.6\pm0.08)$ eV derived by D'Andrade *et al.*[8] for $E^{ox}=0.49\pm0.05$ eV referenced to ferrocene. The lowest unoccupied molecular orbital (LUMO) levels were estimated from ionization potentials and electronic absorption bands. Their values are within ±0.1 eV, in agreement with those reported previously for TPD (Ref. 9) and CBP.[10] Device characterization was carried out in argon atmosphere at room temperature. The spectral characteristics of the materials and devices under study were measured with a StellarNet spectroradiometer. The current-voltage characteristics of the devices were measured with a Keithley Source-Measure unit model 236 under continuous operation mode, while the light output power was measured with an EG&G power meter.

Figure 2 compares the PL and EL spectra of neat PtL^2Cl emitters. Both show only a broad featureless band extending from 620 to 760 nm with a full width at half maximum of 140 nm and a peak at about 700 nm, corresponding to the Commision Internationale de L'Eclairage coordinates of $x\approx0.67$ and $y\approx0.33$. The infrared portion (above 700 nm) constitutes about 50% of the total emission output. However, when this ratio is accounted for, the emission efficiency at λ=770 nm (within a 10 nm span) amounts to ≈7% ph/e at 2 mA/cm^2 and is much higher than that for molecular electrophosphorescence peaking at the same λ, at which it does not exceed 4.5% ph/e at the same current density.[5]

Figure 3 shows the EL intensity and driving current density of the device from Fig. 1 as a function of applied voltage for different cathodes. From this figure, it is clear that the devices with thin buffer layers of LiF and Pb(IV)O_2 performed much better than those with Al and Ca cathodes, respectively. In each case, the presence of the buffer layer

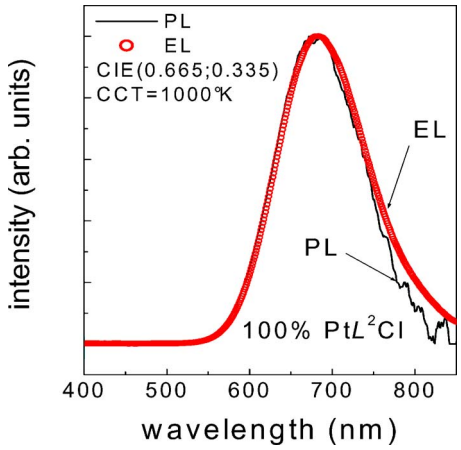

FIG. 2. (Color online) EL and PL (at $\lambda_{exc}=350$ nm) spectra of neat PtL^2Cl films. CIE coordinates and correlated color temperature (CCT) are given in the upper left corner of the figure.

resulted in a shift of the operating voltage to lower values, and in a higher EL output, than those of the devices without buffer layers. The operating voltage for devices with a Ca/Pb(IV)O_2 cathode is found to be nearly half of that for the LEDs with Ca alone. The maximum EL output of 25 mW/cm^2 for the Ca/Pb(IV)O_2 cathode is obtained, with the level ten times higher than that for a device with the Ca cathode alone.

A comparison between efficiency measures of devices with and without thin film buffers is shown in Fig. 4. The data indicate that though the large current density enhancement in performance of the Ca/Pb(IV)O_2 devices is not as strongly pronounced as that for Al/LiF, the Ca/Pb(IV)O_2 devices reveal the highest absolute values of the EL QE ($14.5\pm0.2\%$ ph/e at a maximum for $j\approx2$ mA/cm^2) and power conversion factor ($\eta=6\%$ at low current densities).

For insight into the origin of the observed great improvements in device performance with the buffer layers, the following processes are of essential relevance: (i) The first process is the elimination of mismatch between the LUMO of OXA and the Fermi level of metals by the LiF buffer, thus enhancing the electron injection.[11,12] This is a thin (<0.5 nm) LiF/H_2O layer, which reduces the electron injec-

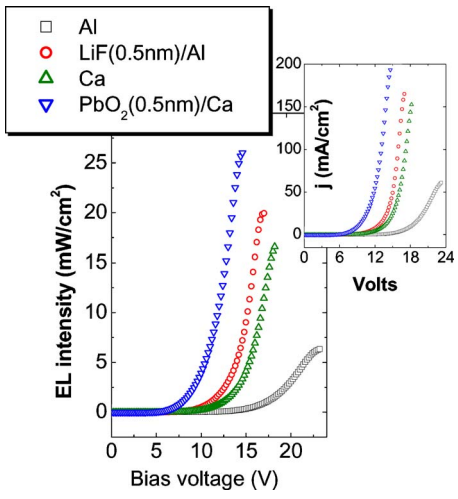

FIG. 3. (Color online) Forward light output (left) and current density (top right) vs bias voltage for different cathodes as indicated in the upper left inset.

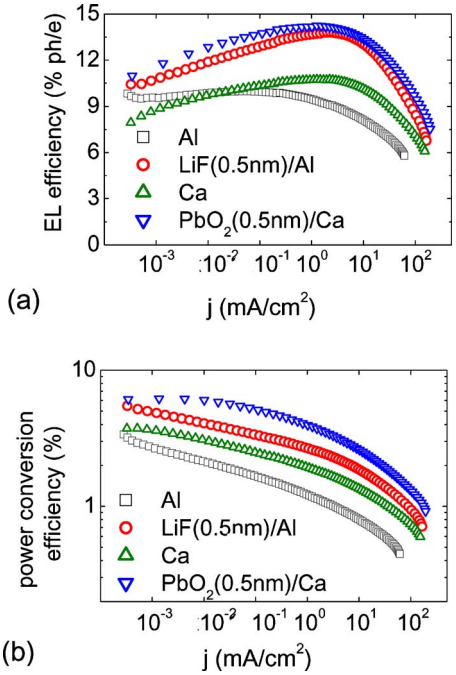

FIG. 4. (Color online) External QE (a) and power conversion efficiency (b) vs drive current density of the present NIR LEDs with different cathodes.

tion barrier down to $\Delta E_{\mathrm{inj}} \approx 0.4$ eV in LEDs with Al cathode.[13] (ii) The second process is an increase of the vacuum level of the metal cathode due to the dipole charge layer,[7,13] which moves its Fermi level toward the LUMO of OXA. No barrier reduction due to H_2O is expected with $Pb(IV)O_2$ since, in contrast to LiF, its hygroscopic properties have not been reported. Instead, an upward shift of ~1 eV of the vacuum level of the Ca cathode may occur because of the surface dipolar layer formed by the tailing of the electron cloud at the surface.[7] As a result, the mismatch between the LUMO of OXA and the Fermi level of Ca increases up to ~1.3 eV. Inserting a thin $Pb(IV)O_2$ layer between Ca and OXA prevents the formation of the dipolar layer leveling off their vacuum levels, and the mismatch gap reduces down to ~0.2–0.3 eV. This would make the $Pb(IV)O_2$/Ca buffer layer more effective in the enhancement of the electron injection than that with the buffer layer LiF of the Al/LiF cathode. The enhanced electron injection results in more electrons available for the recombination at the CBP/PtL^2Cl interface. As a consequence, the recombination zone width (w) reduces, leading to the increased recombination probability,[14] $P_R=(1+w/d_e)^{-1}$, where d_e is the thickness of the EML, and thus to the enhanced EL output. Locating the center of the recombination zone at 45 nm from the cathode in the absence and at 45 nm $< x_R <$ 60 nm in the presence of the $Pb(IV)O_2$ buffer layer generates a 2% change of the triplets yield (P_T) at most. Thus, the observed 40% increase of the $\varphi_{\mathrm{EL}}^{\mathrm{ext}}$ at 1 mA/cm^2 (see Fig. 4) is due to the change of P_R rather than of P_T. This increase requires a 40% shortening of the recombination zone that is 12 nm thick, which is expected with the Ca/$Pb(IV)O_2$ cathode instead of the 30 nm layer without the buffer. (iii) The third process is the reduction of the emission efficiency due to a shortening of the singlet exciton lifetime caused by the dipole-metal cathode energy transfer at a distance ℓ with a rate $k_{\mathrm{ET}} \sim \ell^{-3}$, which reduces the lifetime (τ) of the excitons located at short dipole-cathode separation $\ell \ll \lambda$,[15] and leads to a decrease in the emission efficiency. A 30% reduction of τ is expected at a 30 nm distance of the emitter to cathode for an isotropic dipole distribution.[15] We note that these are primary produced large dipole moment molecular singlet excitons that interact efficiently with the metal electrons. The narrowing of the recomination zone moves "the center of gravity" of the emissive species away from the cathode, reducing the quenching rate k_{ET}, thus increasing probability of the formation of emissive triplets in the recombination process,[1,14] $P_T=(3/4)+(1/4)(1+k_{\mathrm{ET}}/k_{\mathrm{ISC}})^{-1}$, where k_{ISC} is the singlet-triplet intersystem crossing rate constant. However, the above indicated narrowing of the recombination zone leads to only a 2% increase of the emissive triplets. Thus, the observed 40% increase of the $\varphi_{\mathrm{EL}}^{\mathrm{ext}}$ at 1 mA/cm^2 (see Fig. 4) is due to the change in P_R rather than of the probability of the formation of triplets.

In summary, we have shown that by variation of the negative electrode, the external QE of a NIR organic LED based on a neat phosphor film excimer emissive layer varies by a factor of more than 1.5. Inserting a buffer layer (0.5 nm thick) of $Pb(IV)O_2$ between the Ca cathode and ETL, we have demonstrated improved device performance and a very high efficiency of $14.5 \pm 0.2\%$ ph/e, which is the highest figure reported for a NIR organic LED to date. Using the buffer layer matches the LUMO of the ETL with the Fermi level of the metal by the elimination of the dipole charge layer formed at the ETL/Ca interface.

We would like to acknowledge the financial support from FIRB Prohect "NODIS" and "LUCI", and European COST Project No. D35-0010-05.

[1] J. Kalinowski, *Organic Light Emitting Diodes: Principles, Characteristics, and Processes* (Dekker, New York, 2005).
[2] B. W. D'Andrade and S. R. Forrest, Adv. Mater. (Weinheim, Ger.) **16**, 1585 (2004).
[3] M. Cocchi, J. Kalinowski, D. Virgili, V. Fattori, S. Develay, and J. A. G. Williams, Appl. Phys. Lett. **90**, 163508 (2007).
[4] M. Cocchi, D. Virgili, V. Fattori, J. A. G. Williams, and J. Kalinowski, Appl. Phys. Lett. **90**, 023506 (2007).
[5] Y. Sun, C. Borek, K. Hanson, P. I. Djurovich, M. E. Thompson, J. Brooks, J. J. Brown, and S. R. Forrest, Appl. Phys. Lett. **90**, 213503 (2007).
[6] M. Cocchi, D. Virgili, V. Fattori, D. L. Rochester, and J. A. G. Williams, Adv. Funct. Mater. **17**, 285 (2007).
[7] H. Ishii, K. Sugiyama, E. Ito, and K. Seki, Adv. Mater. (Weinheim, Ger.) **11**, 605 (1999).
[8] B. W. D'Andrade, S. Datta, S. R. Forrest, P. Djurovich, E. Polikarpov, and M. E. Thompson, Org. Electron. **6**, 11 (2005).
[9] H. Ogawa, R. Okuda, and Y. Shirota, Appl. Phys. A: Mater. Sci. Process. **67**, 599 (1998).
[10] M. A. Baldo and S. R. Forrest, Phys. Rev. B **62**, 10958 (2000).
[11] F. Li, H. Tang, J. Anderegg, and J. Shinar, Appl. Phys. Lett. **70**, 1233 (1997).
[12] G. E. Jabbour, Y. Kawabe, S. E. Shaheen, J. F. Wang, M. M. Morrell, B. Kippelen, and N. Peyghambarian, Appl. Phys. Lett. **71**, 1762 (1997).
[13] R. Schlaf, B. A. Parkinson, P. A. Lee, K. W. Nebesny, G. Jabbour, B. Kippelen, N. Peyghambarian, and N. R. Armstrong, J. Appl. Phys. **84**, 6729 (1998).
[14] J. Kalinowski, J. Phys. D **32**, R179 (1999).
[15] M.-H. Lu and J. C. Sturm, J. Appl. Phys. **91**, 595 (2002).